CRISPR/Cas9 DNA synthesis disruption as a tool to control cell proliferation in vitro and in vivo

Rocio Sartori Maldonado[1], Hossam Montaser[1], Inkeri Soppa[1], Melanie Balaz[1], Henri Puttonen[4], Solja Eurola[1], Timo Otonkoski[1,2], Jonna Saarimäki-Vire[1], Kirmo Wartiovaara[1,3].

Affiliations:

1- Stem Cells and Metabolism Research Program, Faculty of Medicine, University of Helsinki, Helsinki, Finland
2- Children's Hospital, University of Helsinki and Helsinki University Hospital, Helsinki, Finland
3- Clinical Genetics, Helsinki University Hospital, Helsinki, Finland
4- Pathology, Helsinki University Hospital, Helsinki, Finland

Abstract

Cell therapies hold a lot of promise for regenerative medicine and gene therapy. However, many living cell products entail a fundamental biological risk of unwanted growth. Here, we describe a novel metabolic safety system to control cell proliferation without exogenous genetic elements. The method allows robust cell culture and manufacture while mitigating the risk of uncontrolled growth of transplanted cells.

Using CRISPR/Cas9, we inactivated the enzyme in charge of the *de novo* thymidylate synthesis (*TYMS*) in several cell lines, including human induced pluripotent stem cells. This resulted in cells that proliferate when supplemented with exogenous dTMP but fail to grow in its absence. Under dTMP supplementation, TYMS$^{-/-}$ hiPSCs produce mature teratomas *in vivo* and differentiate normally into potentially therapeutic cell types, such us pancreatic beta cells. After terminal differentiation, the cells no longer require dTMP to remain functional, as seen by prolonged *in vivo* production of human insulin in mice.

Introduction

Somatic cell therapies offer new possibilities for previously untreatable or challenging medical conditions. Among the cell types used in such therapies, induced pluripotent stem cells (hiPSCs) have garnered significant attention due to their availability from patient-specific somatic cells[1,2] and their capability to differentiate into potentially therapeutic cell lineages, such as glucose-responsive insulin secreting pancreatic islets[3]. Furthermore, the improved technologies for gene transfer and genome editing enable the development of genetically modified cell-based therapies with enhanced therapeutic potential[4–6].

The use of hiPSC offers several advantages over mesenchymal and embryonic stem cells (MSC and ESC, respectively). hiPSCs circumvent ethical concerns associated with the embryo derived ESCs[7,8]. Unlike donor-derived MSCs and ESCs, hiPSCs' patient-specificity minimizes the risk of immune rejection and graft-versus-host disease[9,10]. Moreover, they can be further genetically modified by silencing or modifying genes involved in, for instance, immune recognition[11]. These features broaden their applications in disease modeling and therapy development, and may enhance their compatibility for allogeneic cell therapies, reducing the need for immunosuppression compared to other cell sources. However, although the universal off-the-shelf cell products decrease the risk for treatment rejection, this diminished immunogenicity can also lead to problematic immune evasion in potential oncogenic events.

On top of creating a biologically useful cells for a desired clinical purpose, a successful commercial therapy product development needs to meet the criteria for safety and manufacture scalability. These two goals, however, often compromise each other, since manufacturing benefits from robust cell growth, but intensive or unlimited proliferation poses a threat when the cells are transferred to patients[12,13].

Attempts to create safer cells for therapy have yielded different strategies[14,15]. These safety systems aim to prevent uncontrolled proliferation or eliminate the transplanted cells if necessary[16,17]. Some of the existing safety strategies include the use of inducible apoptotic systems, suicide genes, antibody-mediated cell depletion, and gene editing-based switches (Table 1). Often, these switches work by reversibly activating or inactivating genes upon exposure to a small molecule (ON- and OFF-switches, respectively). However, most of them are transgenic, could be silenced or genetically altered, take long time to work, derive from viruses, cause neurotoxicity and/or present rapid remission[15,18].

60 In this context, we envisioned the generation of an *endogenous* safety strategy, by
61 disrupting a key metabolic gene, whose function can be compensated with a dispensable
62 compound. Using CRISPR/Cas9, we genetically inactivated thymidylate synthase (*TYMS*), the
63 only known enzyme in charge of the *de novo* thymidylate (dTMP) synthesis[19]. This knock-out
64 generates rescuable auxothrophy towards thymidine and restricts the synthesis of DNA,
65 without altering normal RNA or protein production (Fig. 1a). This means that dividing cells
66 depend on external supplementation of thymidine to proliferate and achieve robust
67 manufacturing of the cells of interest. However, once the cells have exited the cell cycle and
68 terminally differentiated, they do not require supplementation to synthesize nucleic acids.
69 While preventing dividing cells from proliferating uncontrollably, this approach does not
70 require the use of small molecules nor the insertion of large transgenic elements, hence it
71 cannot be silenced; and it does not result leaky or immunogenic.
72 Our results provide evidence that the culture and proliferation of *TYMS*$^{-/-}$ cells can be
73 regulated with exogenous dTMP *in vitro* and *in vivo*. Furthermore, the characterization and
74 differentiation of *TYMS*$^{-/-}$ hiPSC show that they provide fully functional source for cell therapy
75 but are unable to sustain unwanted proliferation.
76

77 ## Results

78 ### *Generation of thymidine-dependent cell proliferation with genome editing.*

79 The human thymidylate synthase (PDB: 5X5D) is evolutionarily highly conserved. The
80 functional enzymatic ligand pocket is encoded by exons 4 (amino acid R175), 5 (P193, C195,
81 Q214, S216, D218, R225) and 6 (H256, Y258)[20]. Therefore, to interrupt TYMS activity, we deleted
82 the exon 5 by targeting both intron 4 and intron 5. (Fig. 1.b, Supplementary Fig. 1a). This
83 depleted the enzyme expression at both mRNA and protein levels (Fig. 1.C, Supplementary Fig.
84 1a-b) in several cell lines.
85
86 We hypothesized that *TYMS*$^{-/-}$ cells could be cultured and manufactured normally with
87 external dTMP supplementation, but they would cease to proliferate in its absence. We
88 followed the growth of *TYMS*$^{-/-}$-iPS (Hel24.3[21]) and immortal cell lines without or with different
89 concentrations of dTMP (from 0.3 µM to 40 µM). The untreated (wild-type, WT) cell lines were
90 used as controls. The results suggest that *TYMS*$^{-/-}$ cells proliferate at a rate comparable to WT

91 when supplemented with thymidine but undergo apoptosis early upon dTMP withdrawal (Fig.
92 1d). Moreover, the *TYMS*$^{-/-}$ -hiPSCs used from here onwards could not sustain growth at
93 physiological concentrations of thymidine (Fig. 1e, 1 µM; reference: 0.5-1.4 µM[22]). Contrarily,
94 WT *TYMS*$^{+/+}$ lines maintain equal growth rate in all tested dTMP concentrations (Supplementary
95 Fig. 1d). Cell cycle analysis by flow cytometry of Hel24.3 *TYMS*$^{-/-}$ cells reveal that in the first 24h
96 of dTMP withdrawal, the cells accumulate in G0-G1 and S-phase, and then, as they should
97 continue to G2, accumulate in the subG0-G1 phase (Supplementary Fig. 1e). In accordance with
98 the reports by Diehl et al[23], this suggests that this nucleotide starvation causes a replicative
99 stress sensed in the S-G2 checkpoint.
100
101 *Knock-out hiPSCs pluripotency and genomic integrity.*
102 The *TYMS*$^{-/-}$-iPS cell lines showed no detrimental effects on the identity or functions of the
103 stem cells, tested by standard pluripotency analysis. The undifferentiated *TYMS*$^{-/-}$-Hel24.3 lines
104 showed positive staining for pluripotency markers Nanog, OCT4, Sox2 and SSEA4 and
105 comparable mRNA expression of Sox2, Nanog and OCT4 to wild-type Hel24.3 (Fig. 2a-b). Their
106 chromosomal integrity remained unaltered by the editing process in prolonged culture, tested
107 in several time points for up to 25 passages (Fig. 2c and Supplementary Fig. 1e). The
108 differentiation into the three germ layers with or without dTMP supplementation revealed that
109 the cells successfully differentiate into ectoderm, mesoderm and endoderm when
110 supplemented with dTMP at the early stages of differentiation (Fig. 2d). Supplementation
111 withdrawal during the first stage produced significantly less embryoid bodies at d14 (Fig. 1e).
112 By day 28, however, all attached cells expressed characteristic markers of the three germ layers
113 (Fig 2.f, Supplementary Fig. 1f). The successful survival in 3D aggregates and differentiation of
114 non-supplemented cells may suggest the recycling of thymidine from apoptotic cells until cell
115 cycle exit.
116
117 *TYMS*$^{-/-}$*-hiPSCs produce teratomas when supplemented in vivo.*
118 To test the behavior of our Hel24.3 *in vivo*, we implanted undifferentiated *TYMS*$^{+/+}$ and *TYMS*$^{-}$
119 $^{/-}$-hiPSC aggregates subcutaneously in mice, with 100 mg/kg/day or without dTMP
120 supplementation in the drinking water (Fig. 3a). After 6 weeks, we analyzed the size,
121 composition, and proliferation of the resulting teratomas (Fig 3b-f).

122 *TYMS*$^{+/+}$-hiPSC produced teratoma-like growth regardless of the thymidine supplementation,
123 while *TYMS*$^{-/-}$-hiPSC produced visible teratomas only under dTMP supplementation (Fig 3B).
124 Without supplementation, only one of the mice presented a small tumor. Histological analysis
125 and immunocytochemistry showed that *TYMS*$^{+/+}$-hiPSC generated dense teratomas with high
126 cellularity (Fig. 3c-d). Contrarily, *TYMS*$^{-/-}$-hiPSC overall produced smaller teratomas. Under the
127 chosen concentration of dTMP, the teratomas were bigger and, although they presented overall
128 lower cellularity than their WT counterparts, we could identify denser areas with differentiated
129 structures, consisting mostly of neural tubules, and epithelial cells. Absence of thymidine
130 supplementation resulted in very cystic tumors with low cellularity, significantly less
131 proliferative cells (Fig. 3.f), and composed mainly of primitive glial, epithelial, and mesenchymal
132 tissue.
133

134 *Non-supplemented knock-out beta cells produce insulin in vitro.*

135 One potential and intensively studied cell-therapy target is diabetes, in which stem cell-
136 derived insulin-producing beta cells act as the therapeutic source of insulin. We evaluated the
137 safety, quality, and function of *TYMS*$^{-/-}$-hiPSC-derived pancreatic islets using well-defined, multi-
138 step protocol for beta cell differentiation (Fig. 4a). We differentiated *TYMS*$^{-/-}$ hiPSCs (Hel24.3)
139 *in vitro*, providing thymidine supplementation (40 µM) until maturation. Non-supplemented
140 wild-type Hel24.3 were used as controls, while non-supplemented *TYMS*$^{-/-}$ cells died by day 2,
141 making further characterization of this condition impossible.
142 We evaluated the progression of the differentiation protocol by flow cytometry, qPCR, and
143 immunostaining of characteristic markers of several maturation stages. Wild-type and *TYMS*$^{-/-}$
144 Hel24.3 cells showed comparable *in vitro* expression of markers at the definitive endoderm
145 stage (CXCR4), S4 (PDX1, NKX6.1) and S7 (insulin – INS, glucagon – GCG, NKX6.1, PDX1, C-
146 peptide) by flow cytometry (Fig. 4b and Supplementary Fig. 2a-b). In transcriptomic analysis by
147 qPCR, we found that both cell lines expressed characteristic markers at stages DE and S4, and
148 markers of mature beta-cells at week 4 of stage 7 (S7W4) (Fig. 4c). Moreover, at stage 7, the
149 *TYMS*$^{-/-}$- derived islets presented significantly lower *TYMS* mRNA levels. By the last stage before
150 implantation (S7W4), our *TYMS*$^{-/-}$-Hel24.3 islets showed normal morphology and comparable
151 percentage of insulin and glucagon expressing cells (Fig. 4D and Supplementary Fig 2C).

152 Accordingly, *TYMS*$^{-/-}$ and *TYMS*$^{+/+}$ Hel24.3 showed similar *in vitro* levels of glucose and KCl
153 induced insulin secretion (Fig. 4e-f).
154 We did not observe differences between *TYMS*$^{+/+}$-hiPSC differentiated with or without dTMP
155 supplementation, suggesting that the addition of dTMP at our working concentrations (up to
156 40 µM) does not affect *TYMS*$^{+/+}$-cells.
157
158 *In vivo function of non-supplemented TYMS*$^{-/-}$*-hiPSC derived differentiated cells.*
159 We next evaluated the function of mature *TYMS*$^{-/-}$ beta cells (S7) *in vivo* by engrafting them
160 under the kidney capsule in immunosuppressed mice without dTMP supplementation. We
161 implanted seven mice with *TYMS*$^{+/+}$-Hel24.3-derived control islets and six with *TYMS*$^{-/-}$-Hel24.3-
162 derived islets, and monitored their body weight, human C-peptide production, and glucose
163 levels for three months (Fig. 5a-c).
164 Both *TYMS*$^{-/-}$ and control islet successfully mature in the first month, produce comparable
165 levels of human C-peptide, and lower the mouse blood glucose closer to human physiological
166 values (Fig. 5a, b). All mice maintained their normal body weights (Fig 5b-c) and showed no
167 signs of other health concerns.
168 Immunohistochemistry of the *TYMS*$^{-/-}$-implanted kidneys showed vascularization in the graft
169 and high percentage of insulin producing cells (Fig. 5d).
170 Additionally, to monitor the proliferation of the cells in the grafts *in vivo* through time (1 and
171 3 months), we supplemented the drinking water of the mice with EdU for 5 days before
172 sacrificing them. Interestingly, while we see reduction on active proliferation in knock-out cells,
173 the uptake of EdU does not seem significantly different. (Fig 5e-f and Supplementary Fig. 3d).
174 This might point to the uptake of EdU as a source of thymidine.
175
176
177 ## Discussion
178 Here, we have developed a method to generate controllable cells without inserting any
179 external genetic elements. By disrupting the only known *de novo* DNA synthesis reaction, we
180 have obtained cells auxotrophic to thymidine. This approach worked in several cell lines and
181 successfully generated cells that require the external administration of thymidine to
182 proliferate. With dTMP supplementation, the cells grow exponentially for undefined periods

183 in culture showing no signs of exhaustion, rendering them useful in commercial biological
184 product development, for example.

185 The *TYMS*$^{-/-}$ hiPSCs retain their pluripotency and differentiate successfully into different
186 cell types. Non-supplemented *TYMS*$^{-/-}$-hiPSC generate small or no teratomas *in vivo* with a
187 significantly lower proliferative index (KI67), pointing to the loss of proliferative capacity of
188 these cells *in vivo* under physiological concentrations of thymidine.

189 Importantly, TYMS activity is required for DNA, but not RNA, synthesis pathways. Hence,
190 we see no functional alterations in the terminally differentiated cells without dTMP
191 supplementations *in vitro* or *in vivo*. The islets survived implantation and proved to
192 successfully secrete human insulin and lower blood glucose up to three months after
193 implantation, without affecting the weight or overall wellbeing of the mice. This suggests that
194 in differentiated postmitotic cells, *TYMS* gene is dispensable.

195 The advances in basic science and technological developments simultaneously pressure
196 and aid pre-clinical studies in their translation to clinical applications. This remains particularly
197 true for the so-called *advanced therapy medicinal products* (ATMP), which include somatic-
198 cell and gene therapies, and tissue-engineered medicines. The regulatory agencies categorize
199 CRISPR-based products as ATMP. Although some of these products have reached the clinical
200 trial stage, the safety concerns arising from altering DNA challenge further applications and
201 the continuity of ongoing trials. In this context, attempts to control the activity and
202 proliferation of the therapeutic cells have proven relatively efficient. These systems, however,
203 have not yet led to the progression of clinical trials to further regulatory phases, possibly due
204 to their complexity or partial/remissive function.

205 We hope that future differentiations of *TYMS*$^{-/-}$ hiPSC into other therapeutic tissues will
206 further confirm the utility of this approach for this form of cell-based therapies. In addition,
207 it is possible to expand this strategy to other therapeutic cell types. Immunotherapies, for
208 instance, currently present the challenge of cells overactivation and overexpansion and are
209 restricted to the use of senescent cells to limit risks. We expect them to benefit from our
210 controllable safety approach, as it would enable and regulate the activity of the therapeutic
211 cells according to supplementation.

212

213

214

215 ## Materials and methods

216

217 **Culture of HEK293 FT, A431, A549, HSC3**

218 We cultured HEK293, epidermoid carcinoma cell line A431, adenocarcinoma human alveolar
219 basal epithelial cells A549, and human oral squamous carcinoma cell line HSC-3 cells in
220 Dulbecco's modified Eagle's medium (DMEM) containing 10% fetal bovine serum (FBS), 100
221 µg/ml penicillin-streptomycin and 2 mM GlutaMAX (all ThermoFisher Scientific). After *TYMS*
222 knock-out, cell media were additionally supplemented with 5-20µM dTMP (ThermoFisher
223 Scientific). We kept the cell lines at 37 °C and 5% CO2, with media change every other day until
224 splitting with TrypLE select. All cell lines tested negative for mycoplasma.

225

226 **Induced Pluripotent Stem cells culture and characterization**

227 Human induced pluripotent stem cell (hiPSC) line Hel24.3 were cultured on Matrigel
228 (Corning) coated plates in E8 medium (ThermoFisher Scientific) and split using 0.5 mM EDTA.
229 We kept the cell lines at 37 °C and 5% CO2, with media change every other day. All cell lines
230 tested negative for mycoplasma. After *TYMS* knock-out, cell media were additionally
231 supplemented with 5-20µM dTMP. The karyotyping was carried out by Ambar Anàlisis
232 Mèdiques (Barcelona, Spain) by G-banding. We treated edited (passage 20 and 45) and non-
233 edited (passage 20) hiPSC with colcemid for 4 h, 37°C, 5% CO2 and proceeded to prepare the
234 cells as recommended by the service provider.

235

236 **Genome editing**

237 To knock-out exon 5, we designed guide RNA targeting intron 4 (I4) and intron 5 (I5) using
238 online tools (https://benchling.com, CRISPOR,[24], supplementary table 1). We generated the
239 sgRNA by incubating 5 min at 95 °C our gRNA (customized Alt-R CRISPR-Cas9 gRNA, iDT) with
240 Alt-R® CRISPR-Cas9 tracrRNA, ATTO™ 550 (iDT).

241 For each stem cell electroporation experiment, we dissociated 2x10^6 cells to single-cells
242 with StemPro Accutase (ThermoFisher Scientific). We complexed the sgAlt-R® S.p. HiFi Cas9
243 Nuclease V3 and and both sgRNA to form the functional ribonucleoprotein (RNP) and delivered
244 this RNP into the cells, along the Alt-R® Cas9 electroporation enhancer (all from integrated DNA
245 Technologies – iDT), by electroporation with Neon transfection systems (1100V, 20ms, 2

246 pulses). Cells were plated onto Matrigel-coated plates containing E8 with 5 µM ROCK inhibitor
247 (Y-27632, Selleckchem) and 20-40 µM dTMP, and incubated at 37 ˚C, 5% CO2.
248 24-48 h after electroporation, we sorted ATTO550 positive cells for monoclonal expansion in
249 E8 with 5 µM ROCK inhibitor, 20-40 µM dTMP and 10% CloneR (StemCell Technologies). The
250 media was refreshed every 72 h until splitting. We individually screened monoclonal colonies
251 by PCR. All PCR products of the selected edited clones were validated by Sanger sequencing,
252 along with the integrity of the top-7 off target sequences (Supplementary table 2).
253
254 **Embryoid body differentiation**
255 To test the pluripotency for embryonal lineage differentiation, we grew the cells until 90-
256 100% confluency and performed embryoid body (EB) differentiation assay as previously
257 described [2]. Final plated EBs were fixed with 4%PFA-PBS and immunostained for characteristic
258 markers of the three germ-layers (see list below).
259
260 **Teratoma assay**
261 Knock-out and wild-type Hel24.3 cells were cultured in ultra-low attachment plates with E8
262 supplemented with 5 µM ROCK inhibitor for 24-48h to form aggregates. The medium for knock-
263 out cells was additionally supplemented with 40 µM dTMP until 2h before implantation. Groups
264 of approximately 500 spheres were collected in syringe cannulas for subcutaneous implantation
265 in the legs of the mice. For half of the mice, the drinking water was supplemented with 100
266 mg/kg/day dTMP. 6-8 weeks post implantation the teratomas were extracted and fixed for
267 immunocytochemistry and hematoxilin-eosin stainings as described below.
268
269 **dTMP auxotrophy**
270 Wild-type and knock-out clones from each cell line were split onto Matrigel coated 6-well
271 plates at a reason of a twenty-five thousand cells per well. Each well contained the
272 corresponding medium for the cell line (see *cell culture*) supplemented with 0 to 2mM dTMP.
273 Cells were washed and media were refreshed daily to clear away dead cells debris and keep the
274 thymidine concentration as constant as possible.
275
276
277

278 **Beta-cell differentiation**

279 The *in vitro* beta cell differentiation was carried out as previously described[3]. Briefly, *TYMS*
280 knock-out and control Hel24.3 iPS cells were seeded onto Matrigel coated 10 cm plates as
281 previously stated. Differentiation protocol was started 24 h post-seeding, when the medium
282 was changed to D0 medium. Both cell lines were supplemented with 0 or 40 µM dTMP until
283 maturation. At stage 7, dTMP was withdrawn or kept until analysis (week 1 to 4 from first day
284 of S7). The media was refreshed every 2-3 days until analysis.

285

286 **Flow cytometry**

287 Stage 4 cells and stage 7 stem cell derived islets (SC-islets) were dissociated with TrypLE for
288 10 min at 37 °C and resuspended in 5% FBS-containing PBS. Fixation and permeabilization were
289 done using Cytofix/Cytoperm (BD Biosciences, catalog no. 554714) for 20 min at RT. Then,
290 samples were incubated overnight with primary antibodies at 4 °C, followed by secondary
291 antibodies for 30 min in RT in Perm/Wash buffer (BD Biosciences, catalog no. 554714)
292 supplemented with 5% FBS. The cells were run on FACSCalibur cytometer (BD Biosciences); data
293 were collected with CellQuest Pro v.4.0.2 (BD Biosciences) and analyzed with FlowJo™ v10.8
294 Software (BD Life Sciences). Antibodies are listed in Supplementary Table 3.

295 For cell cycle analysis, wild type and knock out hiPSC were plated overnight on 6 well plates
296 containing E8 supplemented with ROCK inhibitor and 20 µM dTMP. Then, the media were
297 refreshed and for some plates the dTMP supplementation was stopped. Cells from individual
298 wells were collected at 0, 2, 4, 10, 16 and 24h after dTMP withdrawal and fixed using 4% PFA in
299 in PBS. The same timepoint were collected for the supplemented plates. After fixation, samples
300 were washed and incubated 30 min with 10 µg/ml DAPI diluted in 1% Triton-X (Sigma-Aldrich)
301 in PBS. Then, they were immediately analyzed using the NovoCyte Quanteon 4025.

302

303 **Insulin secretion analysis *in vitro***

304 For static analysis of insulin secretion, a total of 30–50 SC-islets were picked and incubated
305 for 90 min in a 12 well plate containing 2.8 mM glucose (G2.8) in Krebs-Ringer buffer (KRB) for
306 equilibration. This was followed by sequential 30-min incubations of G2.8, 16.8 mM glucose
307 (G16.8) and G2.8+ 30 mM KCl in KRB. After each incubation, 200uL samples were taken for
308 further insulin analysis. Once all samples were taken, the islets were collected for DNA
309 quantification. Dynamic insulin secretion test was carried out using a perifusion apparatus

310 (Brandel Suprafusion SF-06) at a 0.25 ml min–1 flow rate, sampling every 4 min. 50 SC-islets
311 were handpicked and perfused with KRB; sample collection started after 90 min of equilibration
312 in G2.8. Insulin content of secretion fractions and SC-islet lysates was analyzed with enzyme-
313 linked immunosorbent assay (ELISA) (Mercodia).
314
315 **Islet *in vivo* characterization**
316 Animal care and experiments were approved by National Animal Experiment Board in
317 Finland (ESAVI/14852/2018). NOD-SCID-Gamma (NSG, Jackson Laboratories, catalog no.
318 0055577) mice were housed in the Biomedicum Helsinki conventional facility in 12 h light/dark
319 cycle and fed standard chow. SC-islet implantations were done following a stablished previously
320 described protocol[3]. Non-fasted blood samples were collected monthly from the saphenous
321 vein for glucose measurement and C-peptide secretion analysis. For further characterization of
322 the SC-islet graft, the engrafted kidney was removed after 1 or 3 months and processed as
323 described below.
324
325 **Immunocytochemistry, immunohistochemistry, and image analysis**
326 Samples from hiPSC were fixed using 4%PFA-PBS for 20 min and permeabilized using 1%
327 Triton-X in PBS. Samples from S4 and S7 SC-islets were fixed with 4% PFA in PBS for 2h, and
328 explanted SC-islet grafts and teratoma-like growths were fixed overnight. After fixation, these
329 samples were embedded in paraffin and sectioned. 5 µm sections were deparaffinized and
330 subjected to HIER in 0.1 mmol l–1 citrate buffer. The cells and tissue slides were blocked with
331 UV-block (Thermo Scientific, catalog no. TA-125-PBQ), and incubated with primary antibodies
332 in 0.1% Tween-20 overnight at 4 °C with the given dilutions (Supplementary Table 3). After
333 washing, secondary antibodies diluted in a similar manner were incubated at RT for 1 h in the
334 presence of Hoechst33342 for nuclear staining.
335 The cells and slides were imaged using Apotome II from a Zeiss AxioImager with the same
336 exposure and export setting used on all slides of each immunostaining. Images were processed
337 in Zen2 Blue Edition v.2 (Zeiss) and analyzed using FiJi [25] or CellProfiler v.4.0[26] with pipelines
338 adapted from a previous report[27]. The same pipeline settings were used on all images of each
339 immunostaining.
340
341 **Protein expression analysis**

342 mRNA expression levels were analyzed by qPCR (supplementary table 4-6). TYMS protein
343 expression was assessed by standard Western blot. Briefly, protein was extracted by using
344 RIPA lysis buffer (20-188, Millipore) supplemented with cOmplete Mini protease and
345 phosphatase inhibitors tablets (Roche). Samples were sonicated (30 sec, %50 duty cycle pulse)
346 and centrifuged for soluble protein extraction. Protein quantification was done using a Pierce
347 BCA protein assay kit (ThermoFisher) and 20-30 µg total protein were run in Mini-PROTEAN
348 TGX Precast gels (#4561033, Bio-Rad). Transfer to a nitrocellulose membrane was done using
349 25V for 6 min in the iBlot2 Gel Transfer device (IB21001, ThermoFisher). Then, the membrane
350 was probed with a rabbit polyclonal primary antibody against TYMS (1:2500, Proteintech;
351 Supplementary table 3). For detection, we used an anti-rabbit HRP-coupled secondary
352 antibody (1:5000, Cell Signalling) and Western ECL substrate (#1705061, Bio-Rad. As a loading
353 control, we probed the membrane with a b-actin-HRP coupled antibody (sc-47778, Santa
354 Cruz).
355
356
357
358 ## References

359 1. Takahashi, K. & Yamanaka, S. Induction of Pluripotent Stem Cells from Mouse
360 Embryonic and Adult Fibroblast Cultures by Defined Factors. *Cell* **126**, 663–676
361 (2006).
362 2. Weltner, J. *et al.* Human pluripotent reprogramming with CRISPR activators. *Nat*
363 *Commun* (2018) doi:10.1038/s41467-018-05067-x.
364 3. Balboa, D., Barsby, T. & Lithovius, V. . Functional, metabolic and transcriptional
365 maturation of human pancreatic islets derived from stem cells. doi:10.1038/s41587-
366 022-01219-z.
367 4. Maldonado, R., Jalil, S. & Wartiovaara, K. Curative gene therapies for rare diseases. *J*
368 *Community Genet* (2020) doi:10.1007/s12687-020-00480-6.
369 5. Maeder, M. L. & Gersbach, C. A. Genome-editing Technologies for Gene and Cell
370 Therapy. (2016) doi:10.1038/mt.2016.10.
371 6. Hsu, P. D., Lander, E. S. & Zhang, F. Development and applications of CRISPR-Cas9 for
372 genome engineering. *Cell* **157**, 1262–1278 (2014).
373 7. Picken, A. *et al.* A Monte Carlo framework for managing biological variability in
374 manufacture of autologous cell therapy from mesenchymal stromal cells therapies.
375 *Cytotherapy* **22**, 227–238 (2020).
376 8. Aboul-Soud, M. A. M., Alzahrani, A. J. & Mahmoud, A. cells Induced Pluripotent Stem
377 Cells (iPSCs)-Roles in Regenerative Therapies, Disease Modelling and Drug Screening.
378 (2021) doi:10.3390/cells10092319.
379 9. Zhao, T., Zhang, Z.-N., Rong, Z. & Xu, Y. Immunogenicity of induced pluripotent stem
380 cells. (2011) doi:10.1038/nature10135.

381 10. Themeli, M. *et al.* Generation of tumor-targeted human T lymphocytes from induced
382 pluripotent stem cells for cancer therapy. (2013) doi:10.1038/nbt.2678.
383 11. Xu, H. *et al.* Targeted Disruption of HLA Genes via CRISPR-Cas9 Generates iPSCs with
384 Enhanced Immune Compatibility. *Cell Stem Cell* **24**, 566-578.e7 (2019).
385 12. Lee, A. S. *et al.* Effects of cell number on teratoma formation by human embryonic
386 stem cells. *Cell Cycle* **8**, 2608–2612 (2009).
387 13. Hentze, H. *et al.* Teratoma formation by human embryonic stem cells: Evaluation of
388 essential parameters for future safety studies. (2009) doi:10.1016/j.scr.2009.02.002.
389 14. Wiebking, V. *et al.* Metabolic engineering generates a transgene-free safety switch for
390 cell therapy. doi:10.1038/s41587-020-0580-6.
391 15. Bonifant, C. L., Jackson, H. J., Brentjens, R. J. & Curran, K. J. Toxicity and management
392 in CAR T-cell therapy. *Mol Ther Oncolytics* **3**, 16011 (2016).
393 16. Lim, T.-T., Geisen, C., Hesse, M., Fleischmann, B. K. & Zimmermann, K. Lentiviral
394 Vector Mediated Thymidine Kinase Expression in Pluripotent Stem Cells Enables
395 Removal of Tumorigenic Cells) Lentiviral Vector Mediated Thymidine Kinase
396 Expression in Pluripotent Stem Cells Enables Removal of Tumorigenic Cells. *PLoS One*
397 **8**, 70543 (2013).
398 17. Chen, F. *et al.* Suicide gene-mediated ablation of tumor-initiating mouse pluripotent
399 stem cells. doi:10.1016/j.biomaterials.2012.11.018.
400 18. Volarevic, V. *et al.* Ethical and Safety Issues of Stem Cell-Based Therapy. *Int. J. Med.*
401 *Sci* **15**, 36–45 (2018).
402 19. Andersona, D. D., Quintero, C. M. & Stovera, P. J. Identification of a de novo
403 thymidylate biosynthesis pathway in mammalian mitochondria. *Proc Natl Acad Sci U S*
404 *A* **108**, 15163–15168 (2011).
405 20. Chen, D., Jansson, A., Sim, D., Larsson, A. & Nordlund, P. Structural analyses of human
406 thymidylate synthase reveal a site that may control conformational switching
407 between active and inactive states. *J Biol Chem* **292**, 13449–13458 (2017).
408 21. Trokovic, R., Weltner, J. & Otonkoski, T. Generation of iPSC line HEL24.3 from human
409 neonatal foreskin fibroblasts. *Stem Cell Res* **15**, 266–268 (2015).
410 22. Traut, T. W. Physiological concentrations of purines and pyrimidines. *Mol Cell*
411 *Biochem* **140**, 1–22 (1994).
412 23. Diehl, F. F. *et al.* Nucleotide imbalance decouples cell growth from cell proliferation.
413 doi:10.1038/s41556-022-00965-1.
414 24. Concordet, J. P. & Haeussler, M. CRISPOR: Intuitive guide selection for CRISPR/Cas9
415 genome editing experiments and screens. *Nucleic Acids Res* (2018)
416 doi:10.1093/nar/gky354.
417 25. Schindelin, J. *et al.* Fiji: an open-source platform for biological-image analysis. *Nature*
418 *Methods 2012 9:7* **9**, 676–682 (2012).
419 26. Stirling, D. R. *et al.* CellProfiler 4: improvements in speed, utility and usability. *BMC*
420 *Bioinformatics* **22**, 1–11 (2021).
421 27. Lithovius, V. *et al.* SUR1-mutant iPS cell-derived islets recapitulate the
422 pathophysiology of congenital hyperinsulinism. *Diabetologia* **64**, 630–640 (2021).
423 28. Karjoo, Z., Chen, X. & Hatefi, A. Progress and Problems with the Use of Suicide Genes
424 for Targeted Cancer Therapy. *Adv Drug Deliv Rev* **99**, 113 (2016).
425 29. Berger, C., Flowers, M. E., Warren, E. H. & Riddell, S. R. Analysis of transgene-specific
426 immune responses that limit the in vivo persistence of adoptively transferred HSV-

427 TK–modified donor T cells after allogeneic hematopoietic cell transplantation. *Blood*
428 **107**, 2294 (2006).
429 30. Sheikh, S., Ernst, D. & Keating, A. Prodrugs and prodrug-activated systems in gene
430 therapy. doi:10.1016/j.ymthe.2021.04.006.
431 31. Sahillioglu, A. C. & Schumacher, T. N. Safety switches for adoptive cell therapy. *Curr*
432 *Opin Immunol* **74**, 190–198 (2022).
433 32. Buil, B. A., Tackenberg, C. & Rust, R. Editing a gateway for cell therapy across the
434 blood–brain barrier. *Brain* **146**, 823 (2023).
435 33. Pellegrini, S., Zamarian, V. & Sordi, V. Strategies to Improve the Safety of iPSC-Derived
436 β Cells for β Cell Replacement in Diabetes. doi:10.3389/ti.2022.10575.
437 34. Tiberghien, P. *et al.* Ganciclovir treatment of herpes simplex thymidine kinase-
438 transduced primary T lymphocytes: an approach for specific in vivo donor T-cell
439 depletion after bone marrow transplantation? *Blood* **84**, 1333–1341 (1994).
440 35. Austin, E. A. & Huber, B. E. A first step in the development of gene therapy for
441 colorectal carcinoma: cloning, sequencing, and expression of Escherichia coli cytosine
442 deaminase. *Mol Pharmacol* **43**, (1993).
443 36. Felmer, R. N. & Clark, J. A. The gene suicide system NTR/CB1954 causes ablation of
444 differentiated 3T3L1 adipocytes by apoptosis. *Biol Res* **37**, 449–460 (2004).
445 37. Gadi, V. K. *et al.* In vivo sensitization of ovarian tumors to chemotherapy by
446 expression of E. coli purine nucleoside phosphorylase in a small fraction of cells. *Gene*
447 *Ther* **7**, 1738–1743 (2000).
448 38. Sato, T. *et al.* Engineered Human tmpk/AZT As a Novel Enzyme/Prodrug Axis for
449 Suicide Gene Therapy. *Molecular Therapy* **15**, 962–970 (2007).
450 39. Serafini, M. *et al.* Characterization of CD20-transduced T lymphocytes as an
451 alternative suicide gene therapy approach for the treatment of graft-versus-host
452 disease. *Hum Gene Ther* **15**, 63–76 (2004).
453 40. Wang, X. *et al.* A transgene-encoded cell surface polypeptide for selection, in vivo
454 tracking, and ablation of engineered cells. *Blood* **118**, 1255–1263 (2011).
455 41. Kieback, E., Charo, J., Sommermeyer, D., Blankenstein, T. & Uckert, W. A safeguard
456 eliminates T cell receptor gene-modified autoreactive T cells after adoptive transfer.
457 *Proc Natl Acad Sci U S A* **105**, 623–628 (2008).
458 42. Birrer, M. J., Moore, K. N., Betella, I. & Bates, R. C. Antibody-Drug Conjugate-Based
459 Therapeutics: State of the Science. *J Natl Cancer Inst* **111**, 538–549 (2019).
460 43. Straathof, K. C. *et al.* An inducible caspase 9 safety switch for T-cell therapy. *Blood*
461 **105**, 4247–4254 (2005).
462 44. Liu, Y. *et al.* Inducible caspase-9 suicide gene under control of endogenous oct4 to
463 safeguard mouse and human pluripotent stem cell therapy. *Mol Ther Methods Clin*
464 *Dev* **24**, 332–341 (2022).
465 45. Wunderlich, S. *et al.* Targeted biallelic integration of an inducible Caspase 9 suicide
466 gene in iPSCs for safer therapies. *Mol Ther Methods Clin Dev* **26**, 84–94 (2022).
467
468
469
470

Conflict of interest

RSM and KW are marked as inventors in a patent application by the University of Helsinki

Aknowledgements

We thank MD Vaino Lithovius for his assistance in image analysis, MSc Sami Jalil for scientific discussion and support, MSc Hazem Ibrahim and MSc Eliisa Vahankangas for assistance with animal care. We thank the Flow cytometry Unit, the Functional Genetics Unit (FuGU) and the Animal facility at Biomedicum Helsinki for their possible contribution to this study. Lastly, we thank Helsinki University Hospital research funding, Paulo Foundation, Signe and Ane Gyllenberg Foundation, Magnus Ehrnrooth Foundation, K. Albin Johansson Foundation, Ida Montin Foundation, Finnish Red Cross Blood Service Research Fund for financial support.

517 Table 1 – Summary table of selected "safety" systems, and potential advantages and
518 disadvantages.
519

Type	Function	Example	Advantages	Disadvantages
Enzyme/Prodrug [28–33]	Transgenes transform prodrug into toxic metabolite	HSV-TK + Ganciclovir[34]	Some have the ability to eliminate the whole graft Could be combined with other strategies Safe Generally efficient	Transgene derive from viruses, bacteria or yeast Immuno-rejection of the therapeutic cells Toxicity of the prodrug Bystander effect Slow activation time Silencing of transgene
		CD+5-FC[35]		
		NTR+CB1954[36]		
		PNP+MEP[37]		
		mTMPK+AZT[38]		
MAb mediated [32,33]	Engineer a gene targeted by an Ab into the transplanted cells	CD20t+Rituximab	Avoid GVHD[39] Efficient Different payloads for ADC	CD20 present in endogenous B cells
		hEGFRt+Cetuximab[40]		
		c-myc tag + Anti-c-myc tag[41]		
		X+ADC anti-X[42]		
Inducible Dimerization[32]	Insertion of a modified Caspase-9. The recruitment sequence is replaced by a dimerization domain of FK506 binding protein	iCas9[43]+CID	Low immunogenicity Inert small molecule Fast action Tested to eliminate iPSC [44]	Silencing of transgene CID resistance[45]
Metabolic	Endogenous disruption of pyrimidine de novo synthesis	UMPS KO[14]	Transgene-free	May affect RNA syntesis

CID: Chemical inducer of dimerization; ADC: antibody–drug conjugate; GVDH: Graft-versus-host disease; CD: cytosine deaminase; NTR: Nitroreductase; HSV-TK: herpes simplex virus thymidine kinase; PNP: purine nucleoside phosphorylase; mTMPK: mutated thymidylate monophosphate kinase; OxPD: Oxazaphosphorine drugs; AZT: azidothymidine

520
521

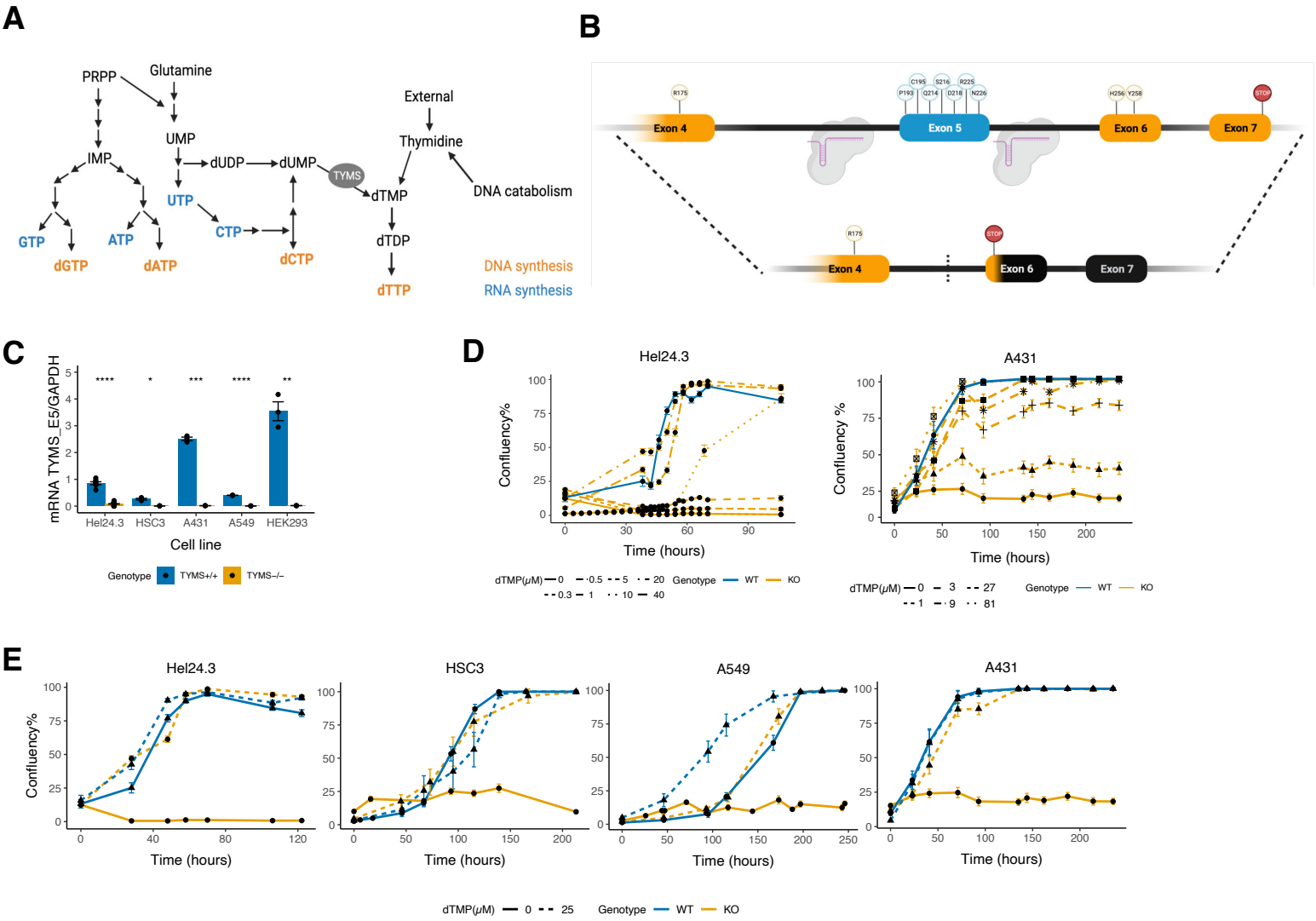

Figure 1. **A.** Diagram showing the nucleotide pathways for DNA (orange) or RNA (blue) synthesis. **B.** Schematic representation of the gene of interest (in TYMS), showing the two gRNAs for our CRISPR/Cas9 approach, and the amino acids that form the active site of the protein over the corresponding exon that code for them. The lower line represents the change of frame upon DNA repair. **C.** TYMS expression in wild-type versus knock-out hiPSC (Hel 24.3), HEK293, A431, A549 and HSC3 (n=3/cell line). Results shown as ratio of TYMS mRNA over GAPDH mRNA contents. **D.** Growth curve of knock-out hiPSC under different concentrations of dTMP. Wild-type without dTMP supplementation (blue) used as control. **E.** Growth curve of wild-type and knock-out hiPSC supplemented with 0 or 25 μM dTMP. Results shown as average confluency per image ? SD. Results shown as average confluency per image ? SD. Statistical significance based on Wilcoxon test; $p < 0.05$ (*), $p < 0.01$ (**), $p < 0.001$ (***), $p < 0.0001$ (****).

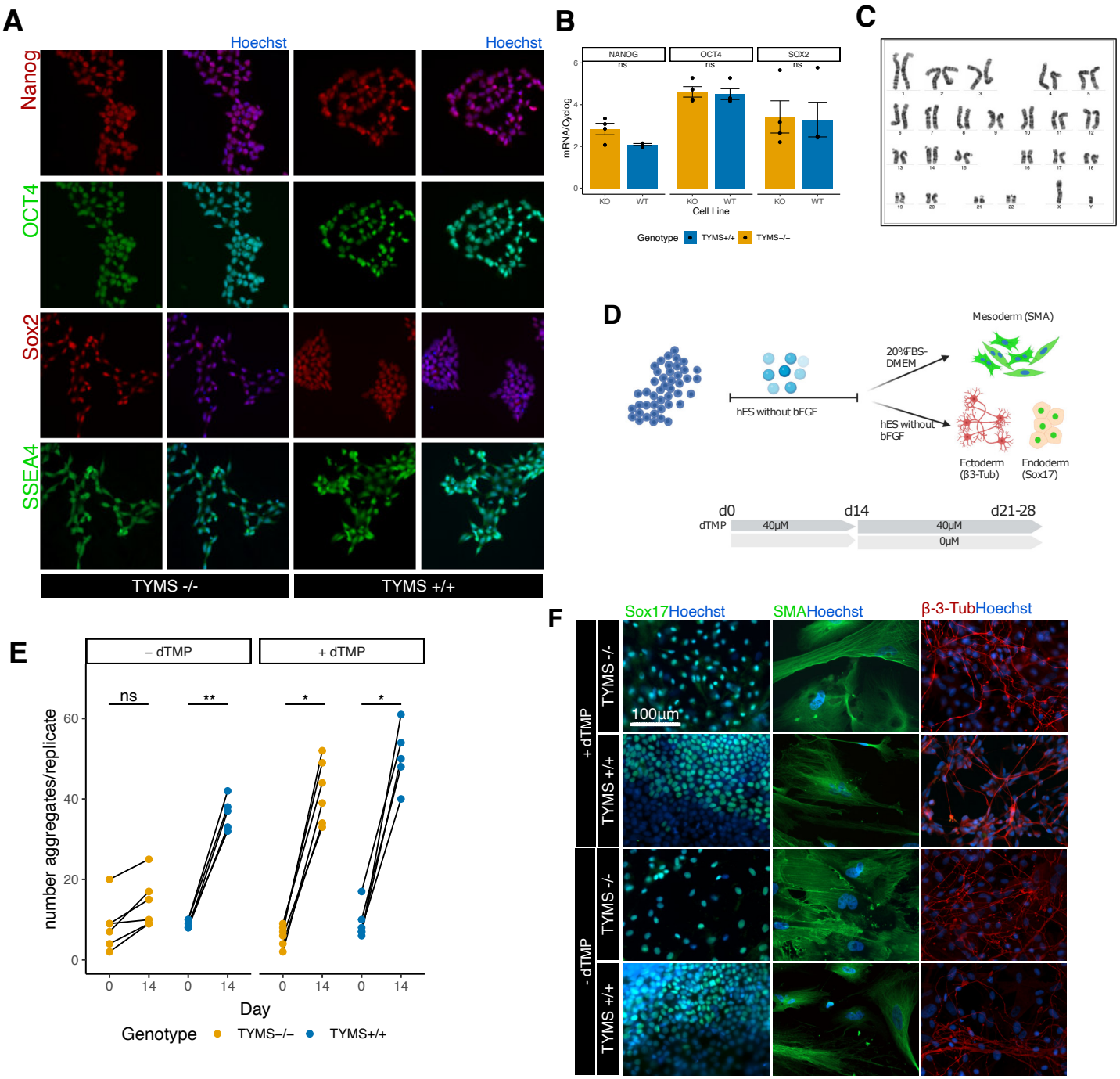

Figure 2. A. hiPSC immunostaining against pluripotency markers NANOG, OCT4, Sox2 and SSEA4. **B.** hiPSC qPCR for expression analysis of pluripotency markers NANOG, OCT4 and Sox2. Results shown as mRNA over Cyclog mRNA. **C.** Karyotype of TYMS-knock-out hiPSC, passage 45. **D.** Graphical representation of trilineage differentiation protocol, dTMP supplementation shown below. **E.** Number of resulting 300 μm aggregates from wild-type and knock-out hiPSC with (+dTMP) and without (-dTMP) supplementation during the first stage of differentiation (day 0 to 14). **F.** Staining against markers for endoderm (Sox17), mesoderm (SMA), and ectoderm (beta-3-tubulin) in cells derived from wild-type and knock-out hiPSC under dTMP supplementation during the first stage of differentiation. Statistical significance in panels B and E is based on Wilcoxon test; $p>0.05$ (ns), $p < 0.05$ (*), $p < 0.01$ (**).

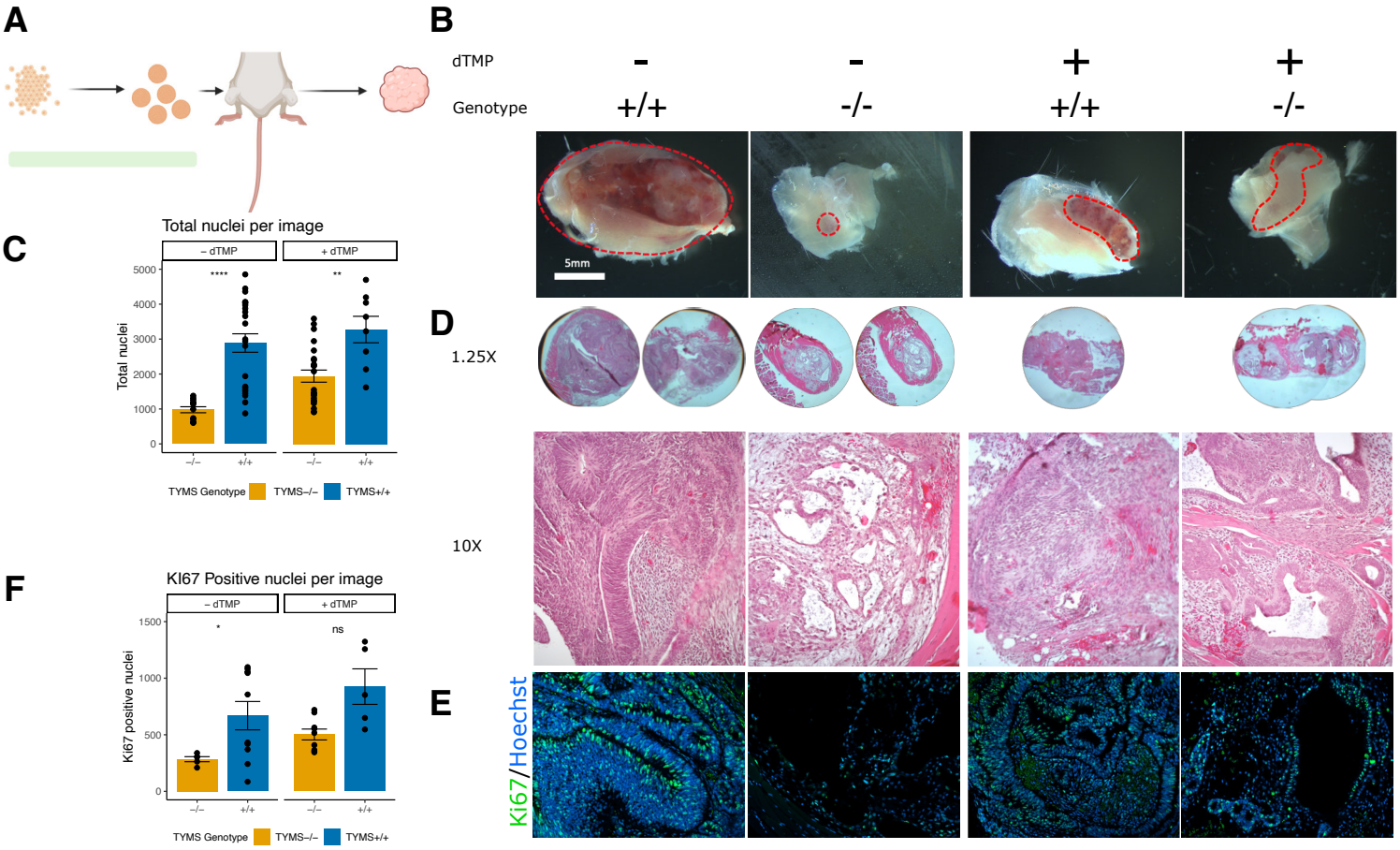

Figure 3. A. Graphical representation of teratoma formation experiment. **B.** Knock-out and wild-type hiPSC-derived teratomas with and without dTMP supplementation as extracted from the mice, before processing for molecular analysis. **C.** Nuclear count of sliced teratomas. **D.** Macro (1.25x) and micro (10x) images of haematoxylin-eosin staining show dense and cystic structures within the tumours, along with structures of the three germ layers (arrows – not there, we need to spot them). **E.** Immunostainings against KI67 (proliferation markers, green) and total nuclei (Hoechst, blue). **F.** Quantification of KI67 positive nuclei from immunostainings. Statistical significance based on Wilcoxon test; $p>0.05$ (ns), $p < 0.05$ (*), $p < 0.01$ (**), $p < 0.001$ (***), $p < 0.0001$ (****).

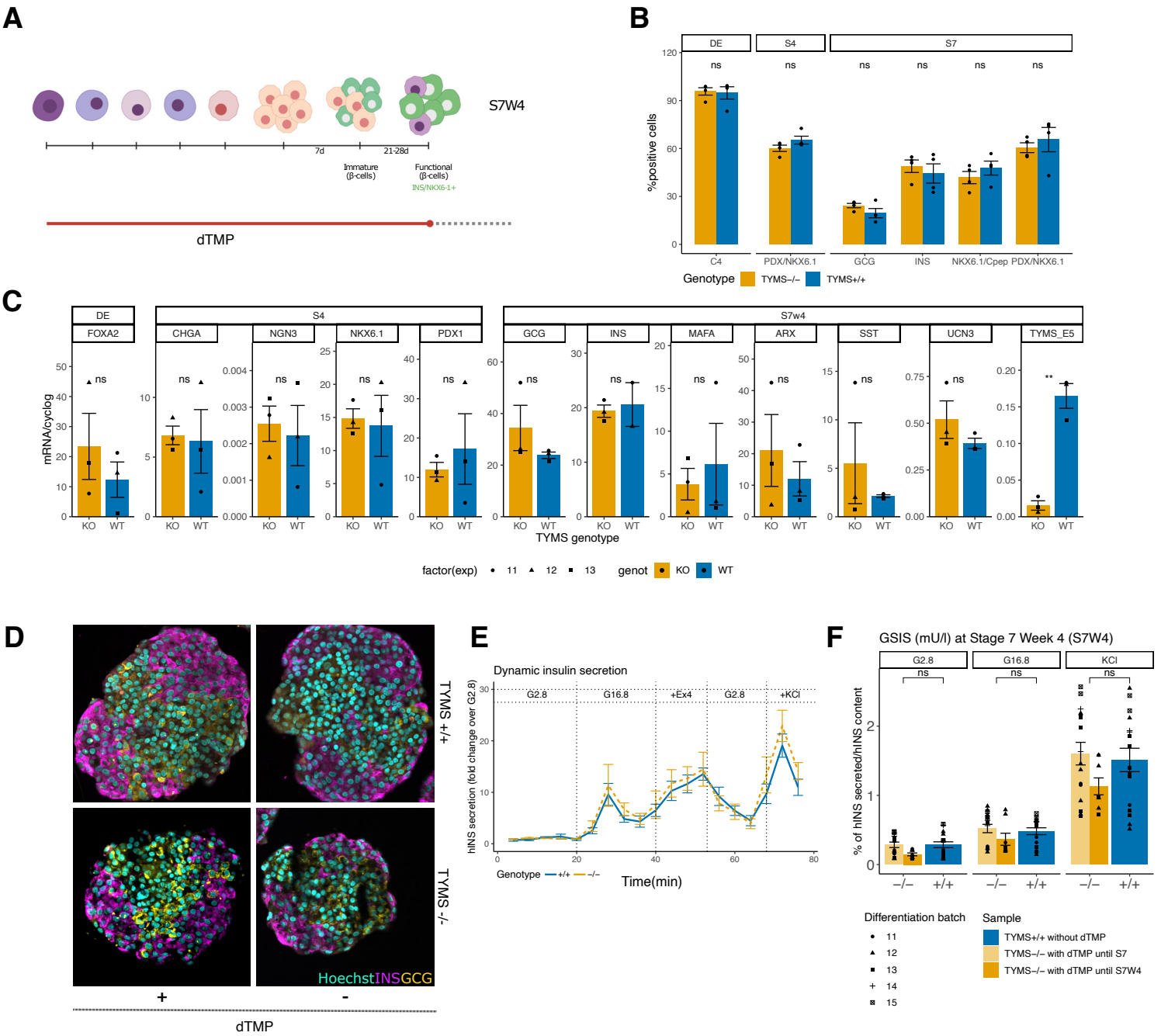

Figure 4. A. Graphical representation of in vitro beta cell differentiation from hiPSC. dTMP supplementation was kept until stage 7 (S7). Following tests were carried out four weeks from stage 7 (S7W4). **B.** Flow cytometry analysis for markers for different stages of differentiation: CXCR4 for definite endoderm stage; NKX6.1 and PDX1 for stage 4; NKX6.1, C-peptide, PDX1, insulin (INS) and glucagon (GCG) for stage 7. **C.** mRNA expression analysis of maturation markers at different stages. Results are shown as each tested mRNA over GAPDH mRNA. **D.** Immunostaining against insulin (INS, magenta) and glucagon (GCG, yellow) in hiPSC-derive islets at stage 7, after 5 days of dTMP supplementation withdrawal. **E.** Dynamic insulin secretion in response to different stimuli (explain). **F.** Insulin secretion in response to low (2.8) and high (16.8) glucose concentration and glucose plus KCl (2.8 KCl). Statistical significance based on Wilcoxon test; $p>0.05$ (ns), $p < 0.05$ (*), $p < 0.01$ (**).

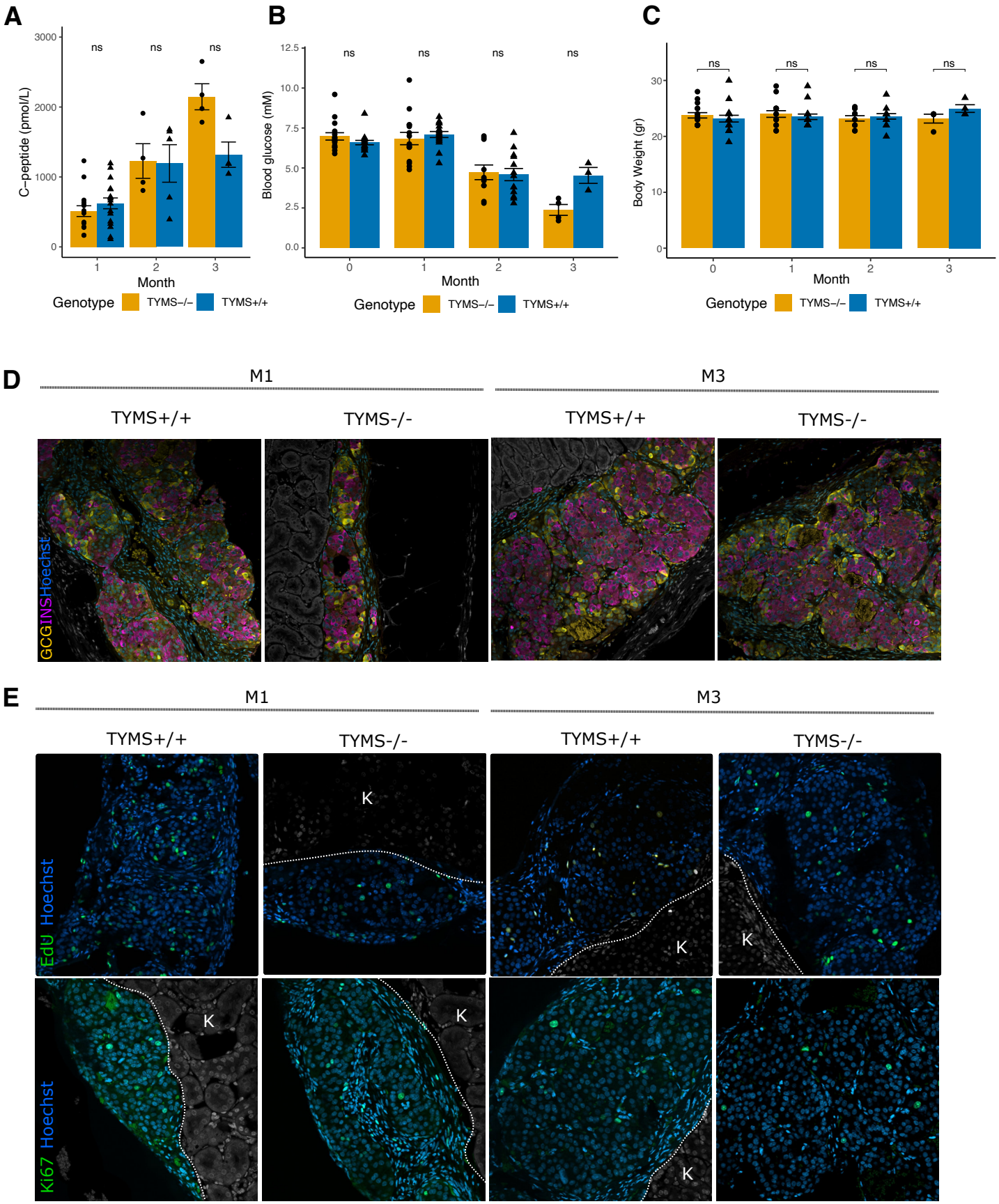

Figure 5. A-C. Follow up of human C-peptide secretion (to serum), blood glucose and mice body weight after 1-, 2- and 3-months from implantation (month 0). **D.** Immunostaining of engrafted kidney 3-months post-implantation. INS (magenta), GCG (yellow). **E.** Immunostaining against EdU and KI67 in grafts after 1 and 3 months. Statistical significance based on Wilcoxon test; p>0.05 (ns).